C. R. Geoscience 344 (2012) 227–238

Contents lists available at SciVerse ScienceDirect

Comptes Rendus Geoscience

www.sciencedirect.com

Tectonics, tectonophysics

Late Cenozoic tectonic stress fields of the Mongolian microplate

Champs de contraintes tectoniques fini-cénozoïques dans la microplaque de Mongolie

Anna V. Parfeevets *, Vladimir A. Sankov

Institute of the Earth's Crust SB RAS, Lermontov Street, 128, Irkutsk 664033, Russia

ARTICLE INFO

Article history:
Received 16 February 2011
Accepted after revision 3 October 2011
Available online 9 February 2012

Written on invitation of the Editorial Board.

Keywords:
Cenozoic
Structural geology
Tectonophysics
Paleostress
Tectonic deformations
Active faults
Mongolia

ABSTRACT

The article deals with the Late Cenozoic fault tectonics and crustal stress state in the Mongolian block (Central and West Mongolia). An analysis was made of the stress field reconstructions, tectonic deformations in active fault zones of the central part of the block (Khangai dome), adjacent uplifts, and intermountain basins, i.e., Mongolian Altai, Gobi Altai, Valley of Lakes, and Khan-Taishir-Nuruu, Khan-Khukhei and Bolnai uplifts. Deformations associated with a general northeast-trending collision compression are concentrated along the periphery of the Mongolian block, the maximum compression occurring on the western and southern block boundaries and giving rise to the right- and left-lateral transpressive structures of Mongolian and Gobi Altai. The deformations associated with the contraction of the Earth's crust affect not only bordering ranges but also the intermountain depressions separating the Gobi and Mongolian Altai from the Khangai and the southern Khangai domes. A variety of deformations in the central Khangai dome is associated with the interaction between extension occurring under dynamic influence of the mantle anomaly and regional north-east compression. Tectonic stiffness of the Khangai block appears to be somewhat favorable to the deformation transfer to its northern termination, i.e., the North Khangai strike-slip fault. This latitudinal zone shows that the compression increases toward the west where it merges with the transpressive structures of the Mongolian Altai, whereas the extension increases toward the east. The formation of releasing bend strike-slip features may be due to the proximity of the Baikal rift zone that resulted from north-west extension associated to a general southwestward movement of the Amur plate.

Mots clés :
Cénozoïque
Géologie structurale
Tectonophysique
Déformations tectoniques
Failles actives
Mongolie

RÉSUMÉ

L'article concerne la tectonique cassante et l'état de contrainte du bloc de Mongolie (Mongolie centrale et occidentale) à la fin du Cénozoïque. L'analyse en a été effectuée à partir de reconstitutions de champs de contraintes, des déformations tectoniques dans les zones de failles actives de la partie centrale du bloc (dôme de Khangai), des surrections adjacentes et des bassins intra-montagneux : Altai de Mongolie, Altai de Gobi, Vallée des Lacs, soulèvements de Khan-Taishir-Nuruu, Khan-Khukhei et Bolnai. Des déformations associées à une compression collisionnelle générale d'orientation nord-est sont concentrées à la périphérie du bloc de Mongolie, la compression maximum s'étant produite aux limites méridionale et occidentale du bloc, et donnant naissance aux structures transpressives dextres et sénestres de l'Altai de Mongolie et de Gobi. Les déformations associées à la contraction de la croûte terrestre n'affectent pas seulement les

* Corresponding author.
E-mail address: aparf@crust.irk.ru (A.V. Parfeevets).

1631-0713/$ – see front matter
doi:10.1016/j.crte.2011.09.009

chaînes bordières, mais aussi les dépressions intra-montagneuses, séparant l'Altai de Mongolie et de Gobi du dôme de Khangai et des dômes du Sud de Khangai. Une variété de déformations dans le Khangai central est associée à l'interaction entre l'extension se produisant sous l'influence dynamique de l'anomalie du manteau et la compression régionale nord-orientale. La rigidité tectonique du bloc de Khangai paraît plutôt favorable au transfert de la déformation jusqu'à son extrémité nord, le décrochement du Kangai Nord : la zone latitudinale montre que la compression augmente vers l'ouest, où elle se confond avec les structures transpressives de l'Altai de Mongolie, tandis que l'extension augmente vers l'est. La formation de décrochements proches de la zone d'inflexion pourrait être due à la proximité de la zone de rift du Baïkal qui a résulté d'une extension nord-occidentale associée à un mouvement général de la plaque Amur vers le sud-ouest.

1. Introduction

As shown by GPS measurements in central Asia (Abdrakhmatov et al., 1996; Calais et al., 2003), the area comprised between the Himalayan collision front and northern part of Eurasia accommodates the north-south to northeast convergence of the Indian and Eurasia plates. It is composed of a mosaic of microplates, such as the Tibet, Dzhungar, Pamir, Afghan, Mongolian, Ordos, Tarim, and Alashan microplates (Zonenshain and Savostin, 1981) (Fig. 1). The inner part of these microplates consists of basins (e.g. Tarim, Alashan, Dzhungaria basins) or high plateaus (Tibet or Pamir plateaus), whereas the microplate boundaries exhibit either fold-and-thrust orogenic belts (Tien Shan, Nan Shan, Mongolian and Gobi Altai and other thrust belts), extended strike-slip faults (Karakorum, Altyn-Tag, Dzhungar, North Khangai and other strike-slip faults) or extension structures such as the Baikal and Shanxi rifts.

This article focuses on the Mongolian microplate and its boundaries, which are viewed as the location of the largest Mongolia historical earthquakes (Fig. 1). Information about tectonic stresses in this region are lacking in spite of numerous articles on active fault kinematics (Cunningham, 2001, 2007; Khilko et al., 1985; Ritz et al., 2003; Walker et al., 2007, 2008), focal mechanisms and mechanical behavior of the crust and the lithosphere (Bayasgalan et al., 2005; Petit et al., 2002), instant crustal movements from GPS measurements (Calais et al., 2003), timing of neotectonic uplifts (De Grave and Van Den Haute, 2002; Vassallo et al., 2007a,b). This work aims at describing the spacial and temporal variations of Late Cenozoic stress states on the basis of structural methods of stress reconstruction.

2. Method

The initial data were collected largely in fault zones indicating Late Cenozoic reactivation. Because neotectonic structural elements commonly develop in older rocks, documenting the age of fracturing and related attributes is an important issue. Outcrops of Cenozoic rocks with well-developed fracture patterns are not frequent. Therefore, the fractures in basement rocks with slickensides devoid of secondary minerals or only with those formed at the surface (calcite, zeolites, iron hydroxides) were selected for reconstruction of the stress fields in the zones of active faults. Slickensides with evidence of chloritization and epidotization were considered to be pre-Cenozoic and as formed at a certain depth, taking into account that erosion in the Late Cenozoic was superficial. Striae in gouges in the crush zones are unambiguous evidence for a Cenozoic age of deformation. Striae and slickenlines superimposed on filled fractures, as well as crosscutting relationships between striae, clearly indicate reactivation of fractures. Measuring fractures in the Cenozoic sedimentary rocks, basalts, and weathered basement are of primary importance. The stress fields reconstructed on the basis of these data are regarded as reference ones for each discrete time interval and location. The paleostress tensors were calculated with the TENSOR program (Delvaux, 1993). The program computes four parameters of the reduced stress tensor: the principal stress axes σ_1 (maximum compression), σ_2 (intermediate compression), σ_3 (minimum compression) and the ratio of principal stress differences $R = (\sigma_2-\sigma_3)/(\sigma_1-\sigma_3)$ defining the shape of the stress ellipsoid. Three major types of the stress regime are recognized: extensional when σ_1 is vertical, strike-slip when σ_2 is vertical, compressive when σ_3 is vertical. The stress regimes vary in function of the stress ratio R as follows: radial extension (σ_1 vertical, $0 < R < 0.25$), pure extension (σ_1 vertical, $0.25 < R < 0.75$), transtension (σ_1 vertical, $0.75 < R < 1$ or σ_2 vertical, $1 > R > 0.75$), pure strike-slip (σ_2 vertical, $0.75 > R > 0.25$), transpression (σ_2 vertical, $0.25 > R > 0$ or σ_3 vertical, $0 < R < 0.25$), pure compression (σ_3 vertical, $0.25 < R < 0.75$) and radial compression (σ_3 vertical, $0.75 < R < 1$). The type of stress regime is also expressed numerically using an index R', ranging from 0.0 to 3.0: $R' = R$, when σ_1 is vertical (extensional stress regime); $R' = 2-R$, when σ_2 is vertical (strike-slip stress regime); $R' = 2 + R$, when σ_3 is vertical (compressive stress regime). This classification (Fig. 2) was proposed by Delvaux et al. (1997) on the basis of Guiraud et al. (1989) classification.

3. Structural analysis and paleostress field reconstructions

3.1. Khangai dome

The core of the Mongolian microplate is the Khangai dome with a low-level seismicity. It comprises areas of basaltic volcanism. The observations showed that normal faults are common in the inner and eastern parts of the

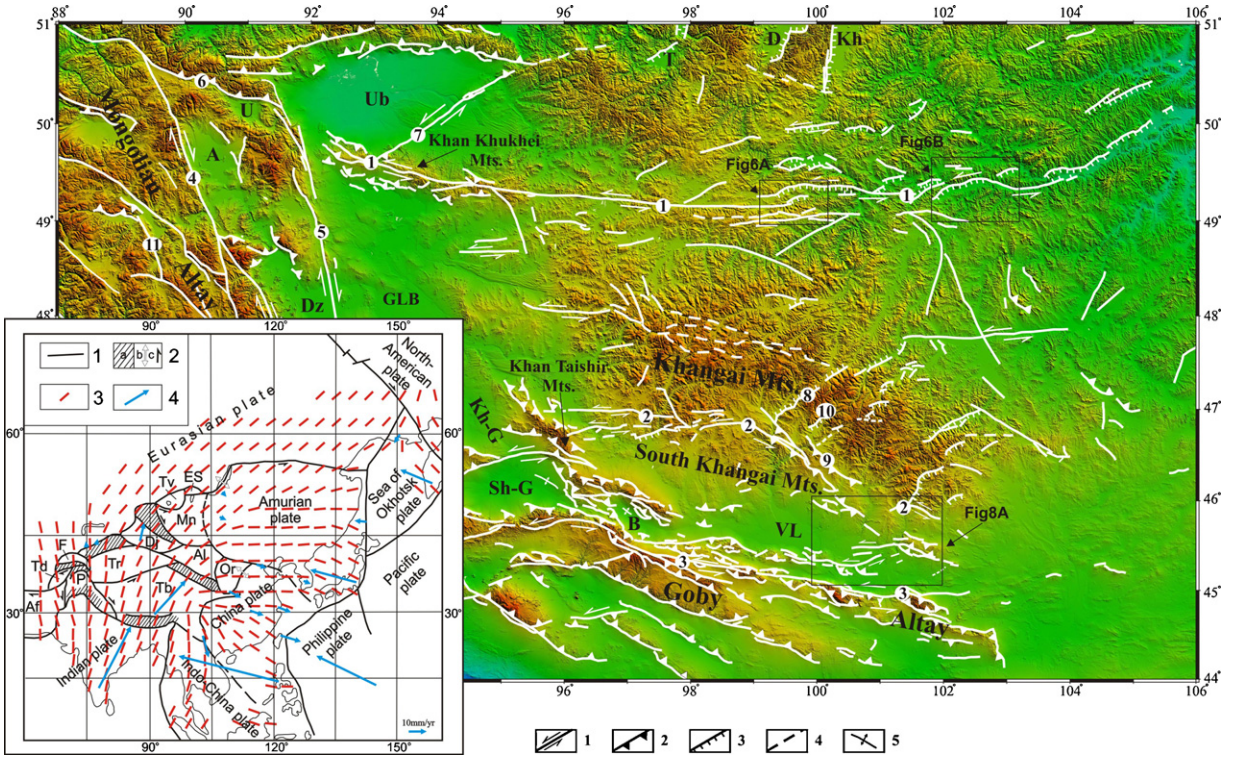

Fig. 1. Shaded relief SRTM-90 digital topography (http://www.nasa.gov) and active faults of Mongolian microplate (authors version with additions from Cunningham, 2007 and Walker et al., 2008). 1 – 4 faults: 1 – strike-slip faults, 2 – reverse faults, 3 – normal faults, 4 – inferred faults; 5 – anticline axes. Letters denote the basins: Ub: Ubsunur; U: Uregnur; Dz: Dzergen; GLB: Great Lakes Basin; Kh-G: Khoisin-Gobi; Sh-G: Shargain-Gobi; B: Beger; VL: Valley of Lakes; T: Terekhol; D: Darkhat; Kh: Khubsugul. Circled figures stand for the faults: 1 – North Khangai, 2 – South Khangai, 3 – Gobi Altai, 4 – Khovd, 5 – Predaltai, 6 – Tsagan-Shibetu, 7 – Erzino-Agardak, 8 – Egijn-Dava, 9 – Bayankhongor, 10 – Mandal. In the insert: Lithosphere plates and microplates of Inner Asia (modified from (Zonenshain, Savostin, 1981). 1 – plate and microplate boundaries; 2 – type of the deformation along plate and microplate boundaries; a – compression, b – extension, c – strike-slip; 3 – orientation of maximum horizontal compressional stress (S_H) smoothed for continental areas with search radius r = 750 km from World Stress Map (Heidbach et al., 2007); 4 – vectors of horizontal present-day movements relative to Eurasian Plate deriving by GPS measurements for some permanent GPS-sites within Asia (Calais et al., 2003). Microplates: Al: Alashan; Af: Afghan; Dj: Dzungarian; Mn: Mongolian; Or: Ordos; P: Pamir; Tr: Tarim; Tb: Tibetan. Smaller blocks: ES: eastern Sayan; Tv: Tuva; Td: Tadzhik; F: Fergana).

Fig. 1. Topographie numérique SRTM-90 à relief ombré (http://www.nasa.gov) et failles actives de la microplaque de Mongolie (Cunningham, 2007 ; Walker et al., 2008). Failles 1 – 4 : 1 – décrochements, 2 – failles inversées, 3 – failles normales, 4 – failles déduites ; 5 – axes d'anticlinaux. Les lettres désignent les bassins : Ub : Ubsunur ; U : Uregnur ; Dz : Dzergen ; GLB : Bassin des grands Lacs ; Kh-G : Khoisin-Gobi ; Sh-G : Shargain-Gobi ; B : Beger ; VL : Vallée des Lacs ; T : Terekhol ; D : Darkhat ; Kh : Khubsugul. Les cercles représentent les failles : 1 – Nord Khangai, 2 – Sud Khangai, 3 – Gobi Altai, 4 – Khovd, 5 – Predaltai, 6 – Tsagan-Shibetu, 7 – Erzino-Agardak, 8 – Egijn-Dava, 9 – Bayankhongor, 10 – Mandal. Dans l'encart : plaques et microplaques lithosphériques d'Asie intérieure (modifié selon Zonenshaim et Savostin, 1981). 1 – limites de plaque et microplaque. 2 – type de déformation le long des limites de plaque et microplaque ; a – compression, b – extension, c – décrochement. Orientation de la contrainte compressionnelle horizontale maximum (S_H) adoucie dans les zones continentales à rayon de détection r = 760 km d'après la carte mondiale des contraintes (Heidbach et al., 2007) ; 4 – vecteurs des mouvements horizontaux actuels relatifs à la Plaque eurasiatique, tirés des mesures GPS pour certains sites GPS permanents en Asie (Calais et al., 2003). Microplaques : Al : Alashan ; Af : Afghan ; Dj : Dzungarian ; Mn : Mongolian ; Or : Ordos ; P : Pamir ; Tr : Tarim ; Tb : Tibetan ; Petits blocs : ES : Sayan Est ; Tv : Tuva ; Td : Tadzhik ; F : Fergana).

Khangai dome, and most of the paleostress field reconstructions correspond to extensive regimes with north-west and north-south extension directions (Fig. 3A, B). The western Khangai dome is dominated by strike-slip displacements that are left-lateral and right-lateral along the east-west and north-west faults, respectively (Walker et al., 2008) (Fig. 1).

The southern and southwestern parts of the Khangai dome exhibits the South Khangai uplift, a relatively low block isolated from the other parts of the Khangai dome by the South Khangai fault (Fig. 1).

The western South Khangai fault has an east-west strike, the fault zone showing displacements of 0.8 to 2 km (Walker et al., 2008). The central segment of South Khangai fault is represented by the north-west trending of Bayankhongor fault that bounds the basin of the same name. The Bayankhongor fault constitutes the current northern boundary of the Early Paleozoic Bayankhongor ophiolite unit, which represents a collision suture between the Baidrag and Khangai pre-Cambrian blocks (Badarch et al., 2002). We consider that this structure was activated during the Neogene-Quaternary time (Nagibina et al., 1975). The Bayankhongor fault gives rise to an ambiguous kinematic interpretation: it is described as a normal fault by Cunningham (2001) whereas it corresponds to a thrust fault for Walker et al. (2007). Most of the paleostress fields reconstructed at various sites along the Bayankhongor fault indicate a compressive regime involving north-east

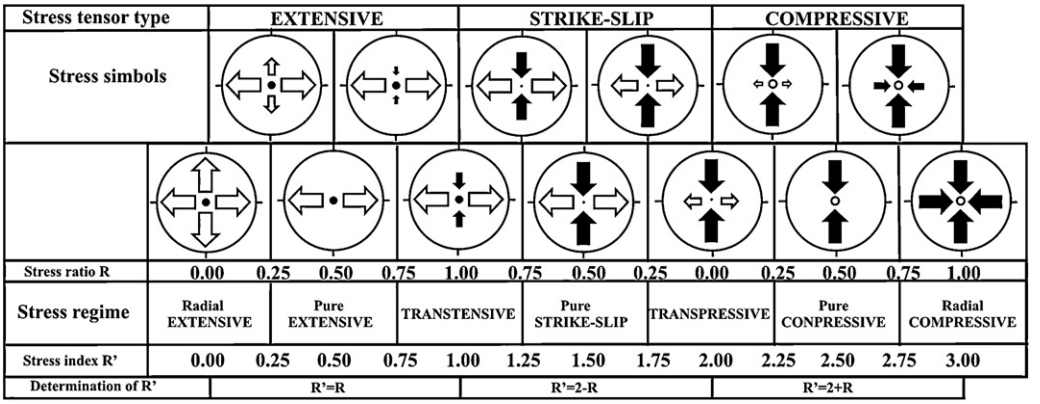

Fig. 2. Types of stress regimes (Delvaux et al., 1997). Stress symbols with horizontal stress axes (S_{Hmax} and S_{Hmin}), as a function of the stress ratio *R*. Their length and colour symbolize the horizontal deviatoric stress magnitude, relative to the isotropic stress (σ_i). White outward arrows: extensional deviatoric stress ($<\sigma_i$). Black inward arrows: compressional deviatoric stress ($>\sigma_i$). The vertical stress (σ_v) is symbolised by a solid circle for extensional regimes ($\sigma_1 = \sigma_v$), a dot for strike-slip regimes ($\sigma_2 = \sigma_v$) or an open circle for compressional regimes ($\sigma_3 = \sigma_v$).

Fig. 2. Types de régimes de contrainte (Delvaux et al., 1997). Les symboles à axes horizontaux de contrainte (S_{Hmax} et S_{Hmin}) sont fonction du rapport de contrainte *R*. Leur longueur et couleur symbolisent la magnitude de contrainte de déviation horizontale, relative à la contrainte isotrope (σ_1). Les flèches blanches dirigées vers l'extérieur représentent la contrainte de déviation d'extension ($<\sigma_i$), les flèches noires dirigées vers l'intérieur, la contrainte de déviation de compression ($>\sigma_i$). La contrainte verticale (σ_v) est symbolisée par un cercle plein pour les régimes en extension ($\sigma_i = \sigma_v$), un point pour les régimes de décrochement ($\sigma_2 = \sigma_v$) ou un cercle vide pour les régimes en compression ($\sigma_3 = \sigma_v$).

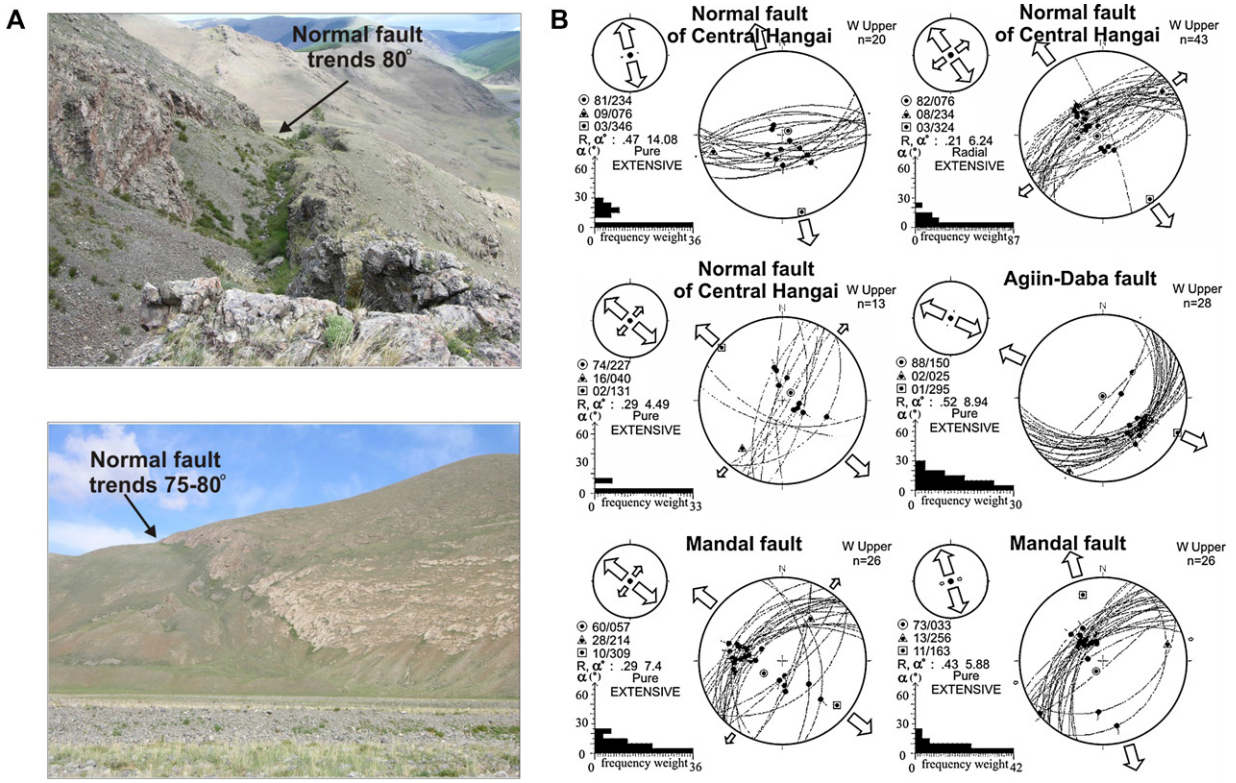

Fig. 3. A. Field photo of normal faults in the central Khangai dome, Urd-Tamir River valley. B. Examples of paleostress reconstructions for the central Khangai dome, including stereograms (Schmidt net, upper hemisphere) with traces of fault planes, observed slip lines and slip senses, and histogram of observed slip theoretical shear deviations for each fault plane and stress map symbol as in Delvaux et al. (1997).

Fig. 3. A. Photo de terrain de failles normales dans le dôme central de Khangai, vallée de la rivière Urd-Tamir. B. Exemples de reconstitutions des paléocontraintes pour le dôme central de Khangai, comportant des stéréogrammes (réseau Schmidt, hémisphère supérieur) avec traces de plans de faille, lignes et sens de glissements observés et histogrammes de déviations de cisaillements théoriques de plissement pour chaque plan de faille et symboles de la carte de contrainte tels que dans Delvaux et al. (1997).

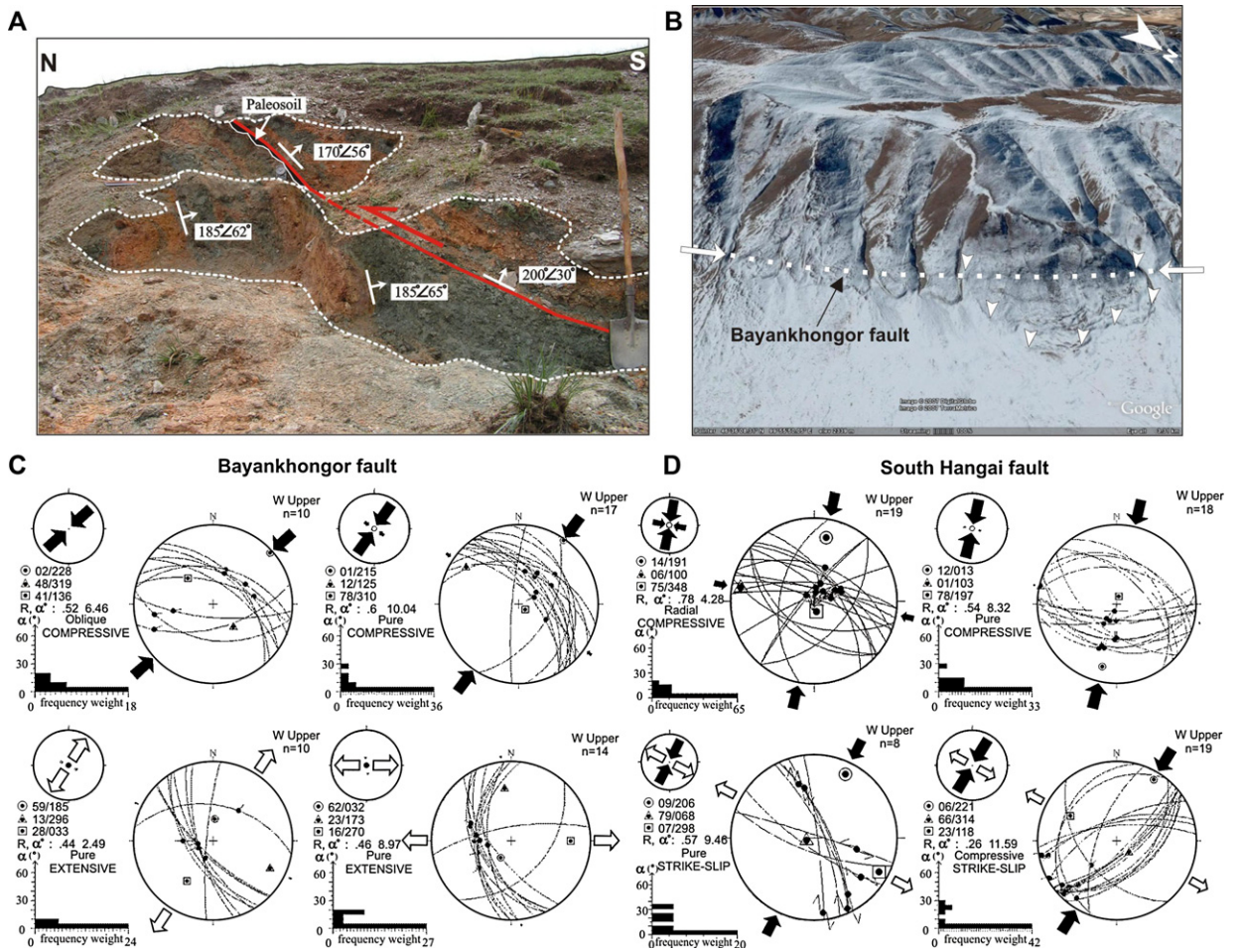

Fig. 4. A. Pleistocene-Holocene thrust deformations in the northwestern Bayankhongor fault zone. The fault plane dip is 200°, angle 30°. B. 3D perspective view generated using Google Earth of the northwestern Bayankhongor fault. C. Examples of paleostress field reconstructions for the Bayankhongor fault. D. Examples of paleostress field reconstructions for the eastern South Khangai fault.

Fig. 4. A. Déformation de charriage Pléistocène-Holocène dans la zone de failles nord-occidentale de Bayankhongor. Le pendage du plan de faille est 200° et l'angle 30°. B. Vue en perspective 3D, générée à partir de Google Earth, de la faille nord-occidentale de Bayankhongor. C. Exemples de reconstitutions de champ de paléocontraintes pour la faille orientale du Sud Kangai.

compression direction (Fig. 4C). Nevertheless, some of the reconstructions show an extensive regime with north-west, north-east to east-west extension direction (Fig. 4C, Fig. 9). This brings up the following question: What is the cause of these discrepancies in the deformation interpretations? We suppose that thrusting may be the determining factor in kinematics of the Bayankhongor fault as exhibited by particular types of thrust faults in the Pleistocene-Holocene sediments (Fig. 4A). Numerous extension directions in paleostress field reconstructions testify to the fact that the extensional regimes are of local character and may be associated with landslides occurring widely in the Bayankhongor fault zone and adjacent rock masses (Fig. 4B). The easternmost WNW trending segment of the South Khangai fault is characterized by the left-lateral strike-slip displacements observed in the large Tatsin-Gol and Sharyn-Gol River valleys. The paleostress field reconstructions demonstrate strike-slip, transpressive and compressive regimes with north-east and north-south compression directions (Fig. 4D).

3.2. Northern boundary of the Mongolian microplate (North Khangai fault)

The North Khangai seismogenic fault zone bounding the Mongolian microplate to the north is extending east-west along the northern slope of the Khangai dome and further west along the Khan-Khukhei Range (Fig. 1). Activation of pre-Cenozoic structures is largely recognized. The fault partly inherits the boundary between Early Paleozoic allochthonous terranes of different origins: Zavhan cratonic terrane and Lake island arc terrane in the south, and Sangelin metamorphic terrane and Agardag backarc/forearc basin terrane in the north (Badarch et al., 2002). With respect to its Late Cenozoic evolution, the fault shows left-lateral strike-slip and reverse-slip displacements. It was activated during the strong Bolnai earthquake

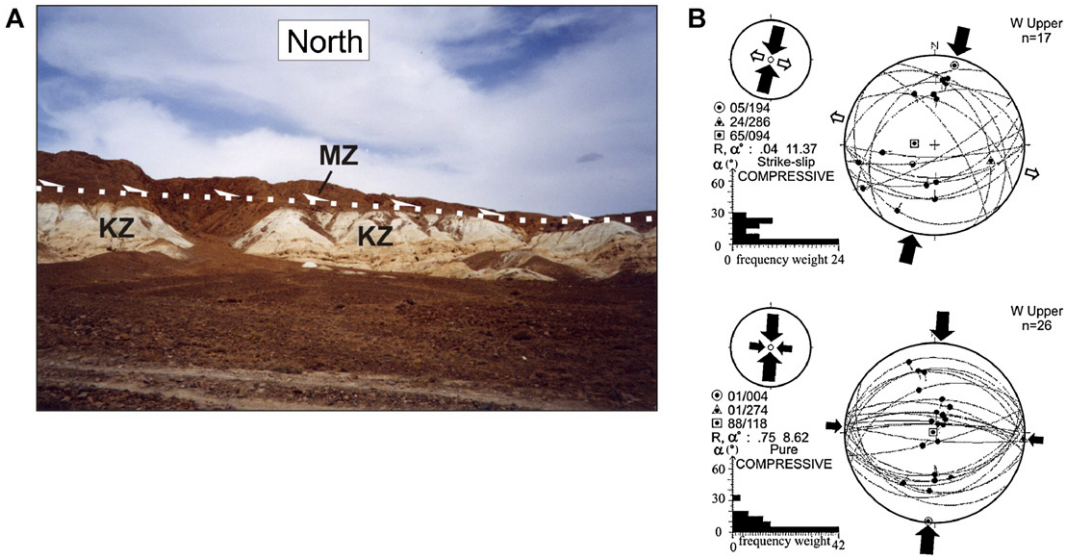

Fig. 5. A. Thrusting of the Mesozoic crystalline rocks over the Cenozoic sediments in the northern shore of Lake Khirgis-Nur (western North Khangai fault). B. Examples of paleostress field reconstructions for the western North Khangai fault.

Fig. 5. A. Charriage de roches cristallines mésozoïques sur des sédiments cénozoïques sur le rivage nord du lac Khirgis-Nur (faille occidentale du Nord Kangai). B. Exemples de reconstitutions de champ de paléocontraintes pour la faille occidentale du Nord Khangai.

($Ms = 8.2$) of July 23, 1905. The North Khangai fault segments have different structure and kinematics. The western segment contains transpression-related structures such as thrusts bordering the major strike-slip fault and deforming the deposits of Cenozoic age (Nagibina et al., 1975) (Fig. 5A). Stress field reconstructions show that compressive and transpressive regimes with a north-south compression axis prevailed (Fig. 5B). The central part of the

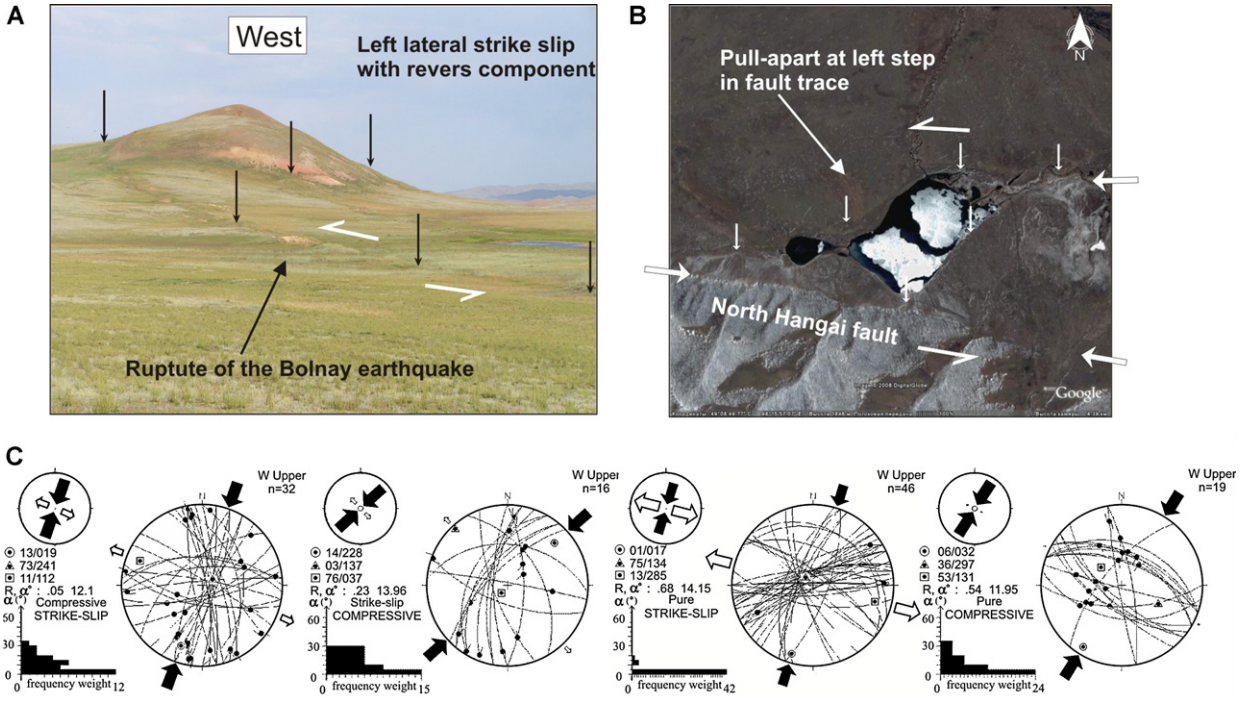

Fig. 6. A. Field photo of "push-up" structure of the central North Khangai fault. B. "Pull-apart" structure (3D perspective view generated using Google Earth of the central North Khangai fault). C. Examples of paleostress field reconstructions for the central North Khangai fault.

Fig. 6. A. Photo de terrain d'une structure en « renflement » de la faille centrale du Nord Khangai. B. Structure en « extension » (Vue en perspective 3D, générée à partir de Google Earth, pour la faille centrale du Nord Khangai). C. Exemples de reconstitutions de champ de paléocontraintes pour la faille centrale du Nord Kanghai.

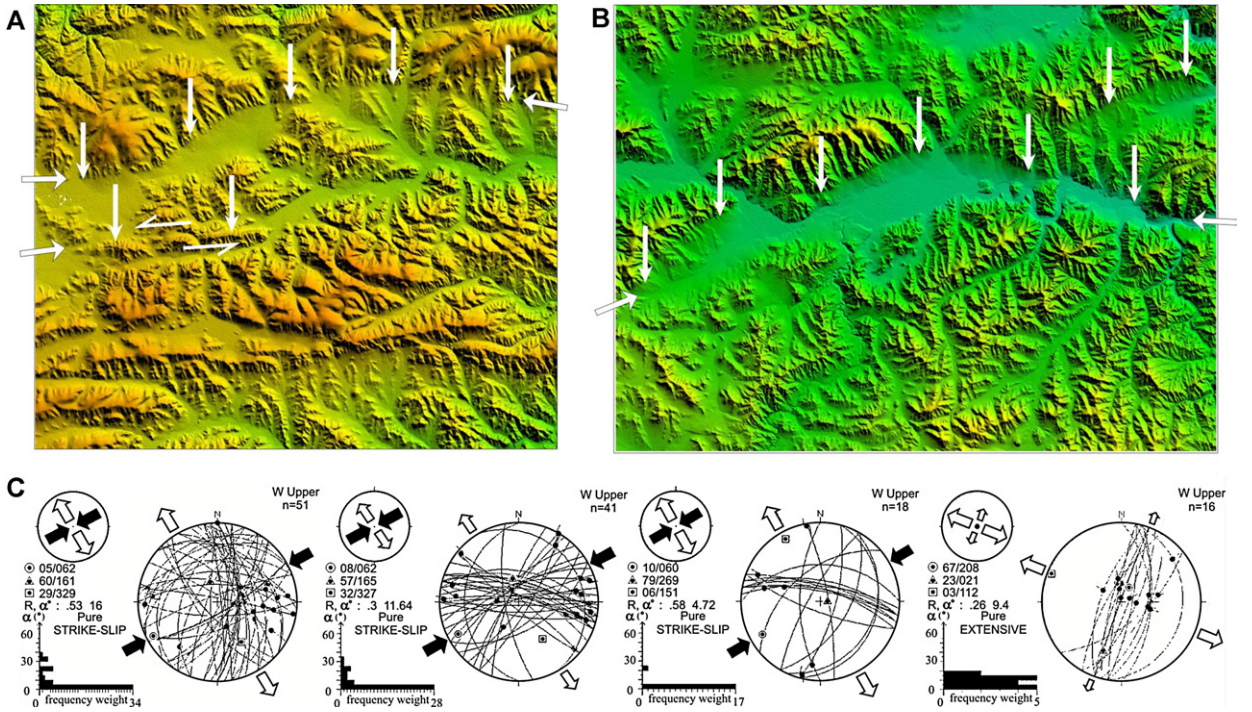

Fig. 7. A–B. Shaded relief SRTM-90 digital topography (http://www.nasa.gov) of the releasing bends of the eastern North Khangai fault. See location of Fig. 6A and 6B in Fig. 1. C. Examples of paleostress field reconstructions for the eastern North Khangai fault.

Fig. 7. A–B. Topographie numérique SRTM-90 à relief ombré (http://www.nasa.gov) des coudes de décrochement de la faille orientale du Nord Khangai. Voir la localisation des Fig. 6A et 6B sur la Fig. 1. C. Exemples de reconstitutions de champ de paléocontraintes pour la faille orientale du Nord Khangai.

fault exhibits "push-up" structures (i.e., longitudinal horsts) and small pull-apart basins along with strike-slip lateral displacements (Fig. 6A, B). The reconstructions are represented by stress tensors of strike-slip, compressive and transpressive regimes with a north-east direction of compression axis (Fig. 6C). We propose that the eastern part of the fault is a releasing-bend strike-slip fault with a set of small north-east trending basins (Fig. 1, Fig. 7A, B). The relevant reconstructions are represented by stress tensors of strike-slip and extensive regimes (Fig. 7C).

3.3. Western and southern boundaries of the Mongolian microplate (Mongolian and Gobi Altai uplifts, Beger basin, Valley of Lakes)

The Mongolian and Gobi Altai uplifts bordering the Mongolian microplate to the west and south are restraining-bend mountain ranges produced by strike-slip and thrust faults as interpreted by Cunningham (2007) and Vassallo et al. (2007b) (Fig. 1). The main active faults of this region (Kobdo, PreAltai and Goby-Altai faults) and also the active faults bounding the Khan-Taishir-Nuruu uplift are inherited boundaries of former Paleozoic allochthonous terranes, recognized by Badarch et al. (2002) as the Altai and Gobi Altai backarc/forearc basin terranes, the Hovd accretionary wedge terrane, Lake Island arc terrane and Darive metamorphic terrane.

The stress reconstructions performed for the Mongolian Altai along NNW trending Khovd and Sagsai fault zones and east-west trending Tsagan-Shibetu fault show compressive and transpressive stress regimes with north-south and north-east compression axes. These successive paleostress regimes induced right-lateral strike-slip displacements of the Khovd and Sagsai faults and reverse displacements of the Tsagan-Shibetu fault zone (Fig. 10), as already recognized by Nagibina et al. (1975).

The Khan-Taishir-Nuruu fault system borders the eponymous range, located in a transition zone between the Mongolian and Gobi Altai structures on one side, and the Khangai dome on the other side (Fig. 1). Transpressive structures of this uplift are connected to the South Khangai fault through a strike-slip faults system. This fault system records Late Cenozoic reverse displacements along the north-west trending faults and reverse and left-lateral strike-slip displacements along the east-west faults. The stress reconstructions in the two fault systems show transpressive to compressive and strike-slip regimes with north-east compression direction, respectively (Fig. 10).

The Beger basin located between the Mongolian Altai and Khan-Taishir-Nuruu uplifts is an intermountain basin bounded by thrust structures (Fig. 1). The edges of the basin are tectonically uplifted and exposed in the foothills of these ranges. The thrust deformation also involves the Cenozoic sedimentary cover (Fig. 8A, B). The stress field reconstructions show compressive and transpressive regimes with north-east compression direction (Fig. 8C).

The Valley of Lakes separates the Gobi Altai and Khangai ranges (Fig. 1). We have studied the ENE faults that may be interpreted as a transition area between the Gobi Altai and South Khangai structures (Fig. 9A). A series of three near

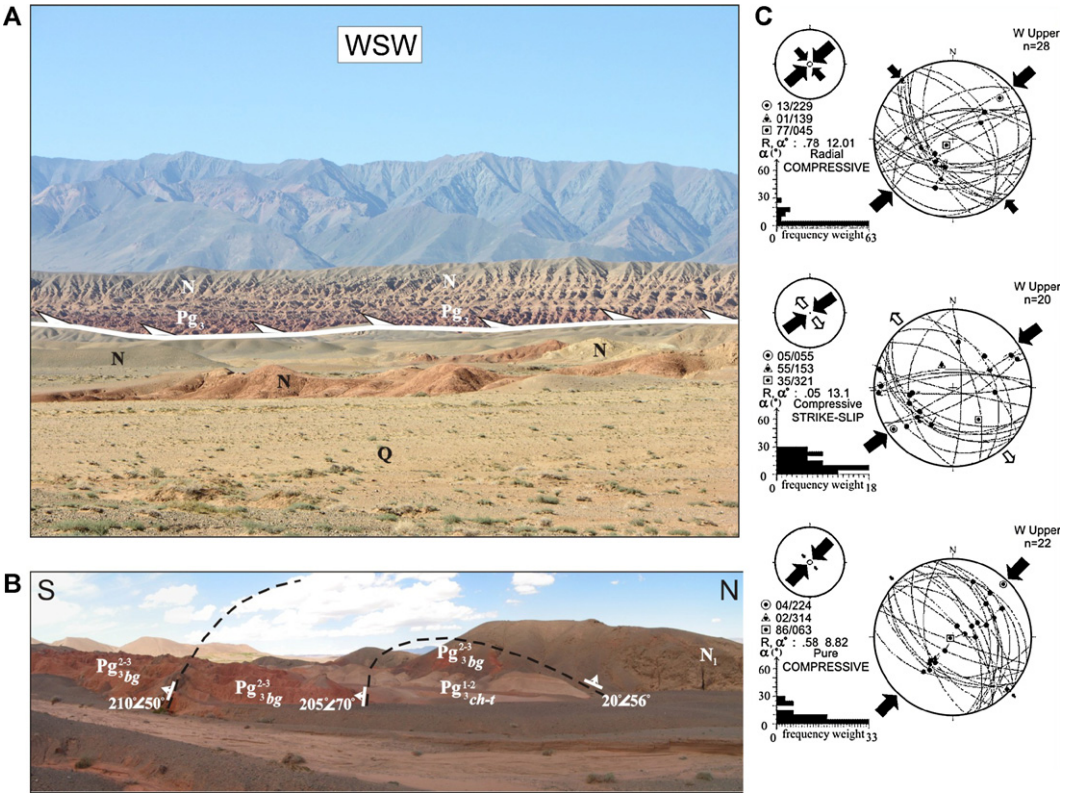

Fig. 8. A. Thrusting in Cenozoic sediments in the southwestern Beger basin. B. Cenozoic anticline (southwestern Beger basin). Low-Middle Oligicene: Pg_3^{1-2} ch-t: Khan-Taishiri suite, Middle-Upper Oligocene: Pg_3^{2-3} bg: Beger suite, Low Miocene: N_1 : Oshin suite. C. Examples of paleostress field reconstructions for active fault zones of the southwestern Beger basin. The names of suites according to Devyatkin (1981). Khan-Taishiri suite is correlated with Ergilin Dzo formation, defined of South-Eastern Gobi. Beger suite corresponds to Hsanda-Gol formation (Berkey and Morris, 1927). Oshin suite is correlated with upper part of Loh formation (Berkey and Morris, 1927).

Fig. 8. A. Charriage de sédiments cénozoïques dans le Sud-Ouest du bassin Beger. B. Anclinal cénozoïque (Sud-Ouest du bassin Beger, Oligocène inférieur et moyen : Pg_3^{1-2} ch-t : suite Khan-Taishiri, Oligocène moyen et supérieur Pg_3^{2-3} bg : suite Beger, Miocène inférieur : N_1 : suite Oshin. C. Exemples de reconstitutions de champ de paléocontraintes pour les zones de failles actives dans le Sud-Ouest du bassin Beger ; les noms des suites sont issus de Devyatkin (1981). La suite Khan-Taishiri est corrélée avec la formation Ergilin Dzo définie dans le Sud-Est du Gobi. La suite Beger correspond à la formation Hsanda-Gol (Berkey and Morris, 1927). La suite Oshin est corrélée avec la partie supérieure de la formation Loh (Berkey and Morris, 1927).

parallel trending faults extends from the Narijn-Kharyn-Nuru uplift in the southwest to the Usgekhijn-Nuru uplift in the northeast. The inner structure of the fault zones is characterized by en-echelon compression features (pressure ridges) and en-echelon extension features (scarps and local basins). The northernmost Dund-Khongor fault zone has a well defined north-facing reverse scarp about 35 m in height. In its western part, there is a pull-apart basin about 1.5×0.8 km in size and about 30 m deep. Deformation features as a whole correspond to left-lateral strike-slip with a reverse component. The strike-slip amplitude reaches 320 m as can be estimated from the displacement of the Late Pleistocene paleo-trace of the Tuin-Gol River near Jinst Somon. The Kholboldzhin-Nur fault zone is extending from the Zagijn-Khundijn-Kholoi area to Kholboldzhin-Nur and Davsan-Nur Lakes. The northern fault wall in the eastern fault segment is made up of down-faulted blocks along the north-east ruptures that also form pull-apart basins. The western fault segment shows the south-facing strike-slip reverse fault scarps that are, on average, 7 m in height. The youngest scarps (possibly of Holocene age) are as high as 2 m. The amplitude of the left-lateral movements along the cumulative surface of the Zagijn-Khundijn-Kholoi area and Tuin-Gol River valley ranges up to 300 m. The Kholboldzhin-Nur fault zone is also associated with some narrow east-west trending anticlines in the Miocene deposits (Fig. 9B). These folds are well expressed in the recent relief. The dip slope of folds indicates the north-east compression direction. Our paleostress reconstructions using tectonic fractures in the Oligocene and Miocene deposits and pre-Cenozoic rocks generally show high prevalence of transpressive and compressive regimes with a north-south or a NNE compression direction (Fig. 9D).

The faults previously named are dynamically associated with the WNW-trending thrust that constitutes the southern border to the Usgekhijn-Nuruu uplift associated to the Khangai structures (Fig. 9A). This thrust was first discovered by E.V. Devyatkin between the Tatsyn-Gol and Khsanda-Gol River valleys (Nagibina et al., 1975). Our geological-structural research along the southern slope of the Usgekhijn-Nuruu uplift provides evidence for the overthrusting of the Paleozoic crystalline rocks over the Late Cenozoic sedimentary units. The

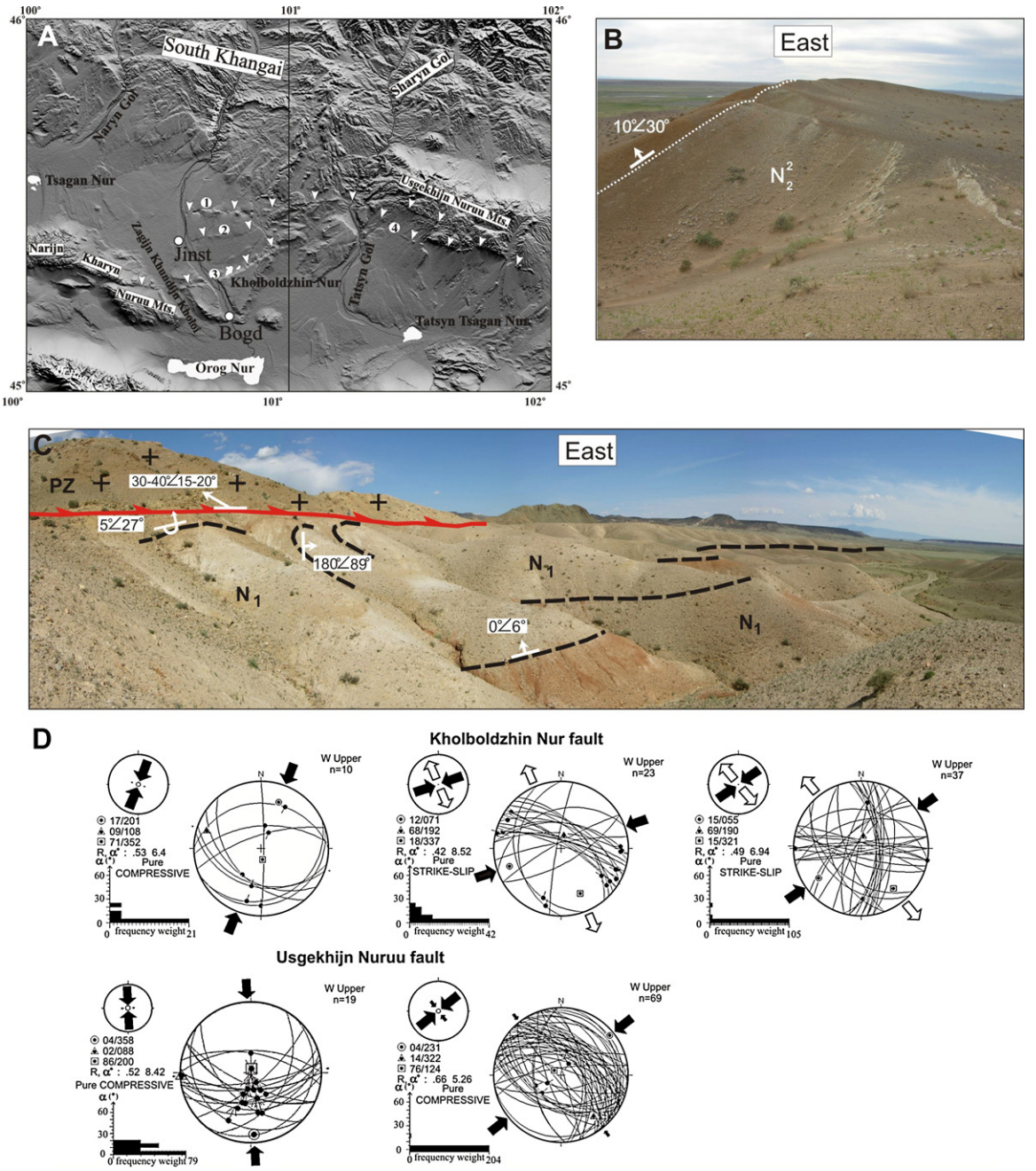

Fig. 9. A. Shaded relief SRTM-90 digital topography (http://www.nasa.gov) of the eastern Valley of Lakes (near Bogd Somon). 1 – Dund-Khongor fault zone, 2 – Jinst fault zone, 3 – Kholboldzhin-Nur fault zone, 4 – Usgekhijn-Nuruu thrust fault. See location of Fig. 10A in Fig. 1. B. Anticline (left bank of Tuin-Gol River). Upper Pliocene: N_2^2 – Tuin-Gol suite (Devyatkin et al., 1989). C. Western Usgekhijn-Nuruu thrust. D. Examples of paleostress field reconstructions for the Kholboldzhin-Nur fault and Usgekhijn-Nuruu thrusts.

Fig. 9. A. Topographie numérique SRTM-90 à relief ombré (http://www.nasa.gov) de la partie orientale de la Vallée des Lacs (près de Bogd Somon). 1 – Zone de failles de Dund-Khongor, 2 – Zone de failles de Jinst, 3 – Zone de failles de Kholdbozhin-Nur, 4 – Décrochement de Usgekhijn-Nuruu. Voir localisation de la Fig. 10A sur Fig. 1. B. Anticlinal (rive droite de la rivière Turin-Gol). Pliocène supérieur : N_2^2 – suite Tuin-Gol (Devyatkin et al., 1989). C. Décrochement occidental Usgekhijn-Nuruu. D. Exemples de reconstitutions de champ de paléocontraintes pour la faille de Kholboldzhin-Nur et les décrochements d'Usgekhijn-Nuruu.

Oligocene and Miocene sediments are interstratified with basaltic flows called the Khsanda-Gol and Loo formations, respectively (Hock et al., 1999). These Cenozoic layers are folded and bent so that sedimentary layering shows reverse dipping beneath the upward-flattening thrust plane (Fig. 9C). The stress field reconstructions indicate a north-south and north-east compression direction (Fig. 9D).

4. Discussion

The active faults of the Mongolian microplate are characterized by variety of kinematics. The strike-slips faults and reverse faults play the main role in accommodating the tectonic movement whereas the thrusts and normal faults play the minor one. Most of these faults are re-activated ancient structures, i.e., boundaries of Paleozoic allochthonous terranes. Brittle deformations affect also inner parts of the blocks. Nice examples of such deformations are present in the eastern part of the Valley of Lakes basin and on the southern and western slopes of the South Khangai uplift.

The data obtained show the prevalence of transpressive fields of tectonic stresses at the periphery of the Mongolian microplate (Fig. 10), which is consistent with earlier studies of active faults kinematics (Cunningham, 2007; Khilko et al., 1985; Ritz et al., 2003; Walker et al., 2007, 2008). Maximum transpressive and compressive deformations are concentrated on the western and southern boundary of the Mongolian and Gobi Altai microplates (Fig. 10, provinces 1, 2, 9, 10, 11), which are characterized by a high level of seismic activity. In addition we observe similarities for the present-day and Late Cenozoic paleostress regimes, with the same directions for the axes of principal normal stresses (Sankov and Parfeevets, 2005).

Reconstructions of Cenozoic paleostresses have been published for the Altai (Delvaux et al., 1995) and the Baikal rift systems (Delvaux et al., 1997; Parfeevets and Sankov, 2006; Sankov et al., 1997). The evolution of Cenozoic stress state is well established for these regions. In particular, temporal changes from extension to transpressive conditions were already described for the Khubsugul basin (Sankov et al., 2004). On the contrary the temporal changes of the crustal stress state were not established for the study area. Possibly compression in north-east direction prevailed since the beginning of the neotectonic activation. According to stratigraphic data (Nagibina et al., 1975) an

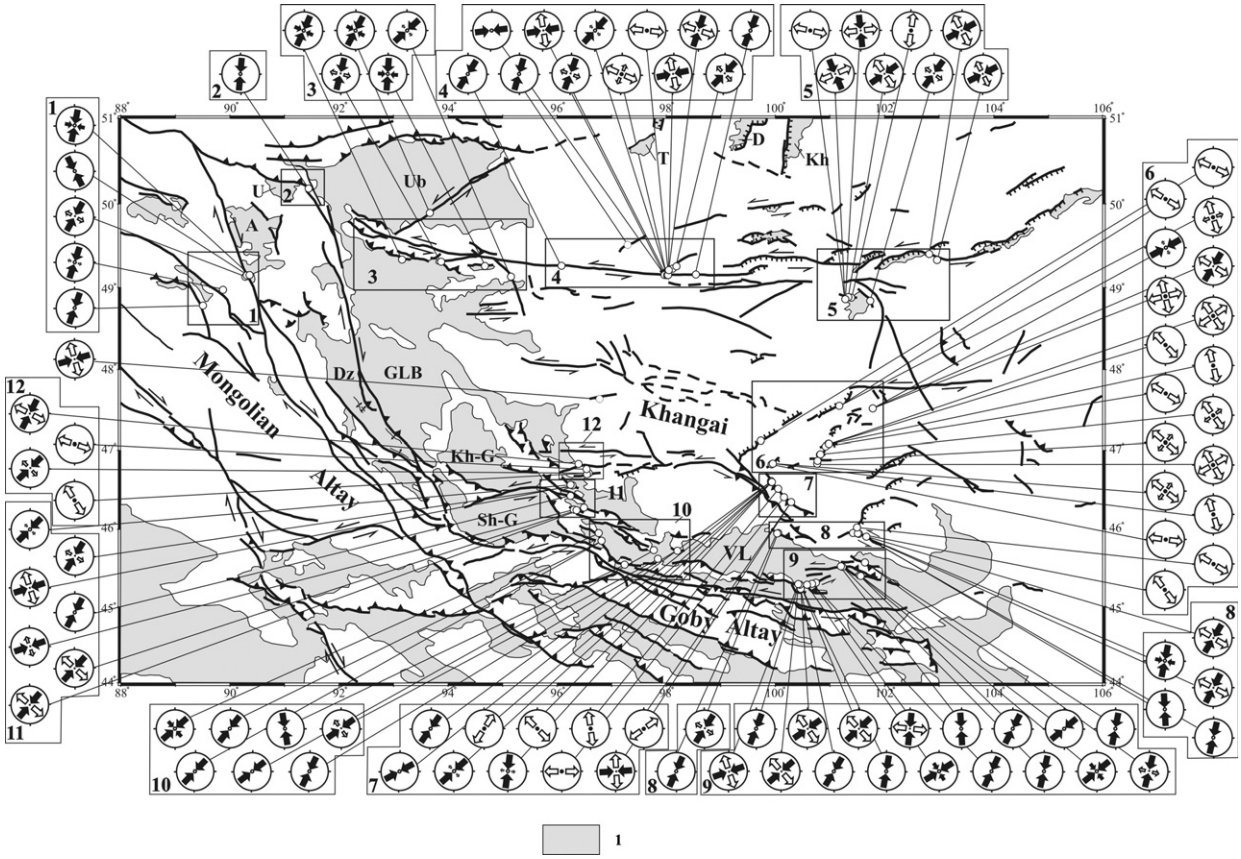

Fig. 10. Stress tensors for the Mongolian microplate. Stress tensors are classified after Delvaux et al. (1997) (Fig. 2). 1 – Cenozoic basins. Squares show the observation site locations: 1 – Hovd and Sagsai faults zone, 2 – Tsagan-Shibetu fault zone, 3 – western North Khangai fault zone, 4 – central North Khangai fault zone, 5 – eastern North Khangai fault zone and Khanuigol basin, 6 – central Khangai dome, 7 – Bayankhongor fault zone, 8 – eastern South Khangai fault, 9 – eastern Valley of Lakes, 10 – Beger basin, 11 – Khan-Taishir-Nuruu uplift, 12 – western South Khangai fault. Other items are the same as in the legend of Fig. 1.

Fig. 10. Tenseurs des contraintes pour la microplaque de Mongolie. Ceux-ci sont classés d'après Delvaux et al. (1997) (Fig. 2). 1 – Bassins cénozoïques. Les carrés montrent la localisation des sites d'observation : 1 – Zone de failles de Hovd et Saozai, 2 – Zone de failles de Tsagan-Shibetu, 3 – Zone occidentale de failles du Nord Khangai, 4 – Zone centrale de failles du Nord Khangai, 5 – Zone orientale de failles du Nord Khangai et du bassin de Khanuigol, 6 – Dôme central de Khangai, 7 – Zone de failles de Bayankhongor, 8 – Faille orientale du Sud Kanghai, 9 – Partie orientale de la vallée des Lacs, 10 – Bassin Beger, 11 – Soulèvement de Khan-Taishir-Nuruu, 12 – Faille occidentale du Sud Khangai. Les autres items sont les mêmes que dans la légende de la Fig. 1.

acceleration of vertical motions in the West Mongolia territory began in post-Miocene time. Recent deformations are recorded both in the uplifted ridges and in the intervening intermountain basins. For example complex deformation has generally occurred in the eastern Valley of Lakes after the deposition of Oligocene-Miocene sediments. Our results suggest a Pliocene onset of tectonic activity in this area together with the active uplift of the Gobi Altai microplate. Apatite thermochronology data (Jolivet et al., 2007; Vassallo et al., 2007a, 2007b) show that the Ikh-Bogd and Baga-Bogd Ranges were uplifted 5 ± 3 My ago.

The prevailing of normal faulting and extensional stress regime in the inner part of the Mongolian microplate is related to intensive uplift of the Khangay dome (Fig. 10, province 6). The dynamic effect of mantle anomaly identified by the seismic tomography (Barruol et al., 2008; Mordvinova et al., 2007) and gravity (Petit et al., 2002) data has facilitated of domal uplift and high magmas permeability of the Khangay crust. In the southern and western parts of the Khangay dome the type of the crustal deformation changes, the overall deformation pattern being characterized there by strike-slip and transpressive features (Fig. 10, provinces 7, 8, 12). These regions are gradually captured by the processes of crustal compression generated by the convergence between India and Eurasia.

The North-Khangay fault is part of the northern boundary of Mongolian microplate. It is characterized by spatial change of the type of crustal deformation from transpressive in the west to strike-slip in the center section, and transtensive in the eastern part (Selenga valley) (Fig. 10, provinces 3, 4, 5). This shows that the influence of the collisional compression weakens eastwards. The extension, related to the divergent motions between North Eurasia and Amur plate (Petit and Fournier, 2005; Zonenshain and Savostin, 1981), plays the major role in the formation of Late Cenozoic structures in the South Trans-Baikal region.

The present-day crustal deformations of Mongolian microplate correspond in general with the paleostress state reconstructed by our structural data. According to the GPS measurements (Calais et al., 2006; Sankov et al., 2005) zones of the horizontal north-east crustal contraction are located along the Mongolian and Gobi Altai ridges. The rate of horizontal deformations decreases in the inner part of the microplate, i.e., the Khangay dome, where contraction is changed to elongation. Along the North-Khangay fault the conditions of crustal contraction in the western segment are also changed by eastwards strike-slip conditions.

5. Conclusion

Our study suggests that:

- maximum deformations associated with the general north-east trend for collision compression are concentrated along the periphery of the Mongolian microplate. The maximum compression is concentrated along its western and southern boundaries, inducing the right- and left-lateral transpressive structures of the Mongolian and Gobi Altai domains;
- crustal shortening occurs not only on the bordering ranges but also in the intermountain depressions separating the Gobi and Mongolian Altai uplifts from the Khangai dome, and on the South Khangai uplift;
- the variety of Khangai deformations is associated with the interaction of extension, driven by the mantle anomaly, and north-east regional compression;
- it seems likely that the rigid Khangai block fosters deformation transfer to its northern termination, i.e., on the seismically active North Khangai strike-slip fault. This latitudinal zone also exhibits a westward increase in compression adjoining the transpressive structures of the Mongolian Altai. It shows also an increase in extension towards the east, where the releasing bends occur. The latter may be associated with the proximity of the central part of the Baikal rift zone, the general southeastward motion of the Amur plate, and related north-west extension direction.

Acknowledgements

The work was carried out with the partial financial support of Russian Foundation for Basic Research (grant no. 11-05-92209) and program of ESD RAS no. 7.7. We thank S.L. Yunga and M. Jolivet for constructive comments and valuable suggestions.

References

Abdrakhmatov, K.Ye., Aldazhanov, S.A., Hager, B.H., Hamburger, M.W., Herring, T.A., Kalabaev, K.B., Makarov, V.I., Molnar, P., Panasyuk, S.V., Prilepin, M.T., Reilinger, R.E., Sadybakasov, I.S., Souter, B.J., Trapeznikov, Yu.A., Tsurkov, V.Ye., Zubovich, A.V., 1996. Relatively construction of the Tien Shan inferred from GPS measurements of present-day crustal deformation rates. Nature 384, 450–457.

Badarch, G., Cunningham, W.D., Windley, B.F., 2002. A new terrane subdivision for Mongolia: Implications for the Phanerozoic crustal growth of central Asia. J. Asian Earth Sci. 21, 87–110.

Barruol, G., Deschamps, A., Déverchère, J., Mordvinova, V.V., Ulziibat, M., Perrot, J., Artemiev, A.A., Dugarmaa, T., Bokelmam, G.H.R., 2008. Upper mantle flow beneath and around the Hangay Dome, central Mongolia. Earth Planet. Sci. Lett. 274, 221–233.

Bayasgalan, A., Jackson, J., McKenzie, D., 2005. Earthquake source parameters, seismogenic thickness and effective elastic thickness in Mongolia. Geophys. J. Int. 163, 1151–1179.

Berkey, C.P., Morris, F.K., 1927. Geology of Mongolia. In: Natural History of Central Asia, 2. American Museum of Natural History, New York, 475 p.

Calais, E., Vergnolle, M., San'kov, V., Lukhnev, A., Miroshnitchenko, A., Amarjargal, S., Déverchère, J., 2003. GPS measurements of crustal deformation in the Baikal-Mongolia area (1994–2002): implications for current kinematics of Asia. J. Geophys. Res. 108 , doi:10.1029/2002JB002373.

Calais, E., Dong, L., Wang, M., Shen, Z., Vergnolle, M., 2006. Continental deformation in Asia from a combined GPS solution. Geophys. Res. Lett. 33, L24319.

Cunningham, W.D., 2001. Cenozoic normal faulting and regional doming in the southern Hangay region, Central Mongolia: implications for the origin of the Baikal rift province. Tectonophysics 331, 389–411.

Cunningham, W.D., 2007. Structural and topographic characteristics of restraining-bend mountain ranges of Altai, Gobi Altai and eastern-most Tien Shan. In: Cunnihgham W.D., & Mann P. (Eds.), Tectonics of strike-slip restraining and releasing bends, Geol. Soc., London, Special Publications, pp. 219–237.

De Grave, J., Van Den Haute, P., 2002. Denudation and cooling of the Lake Teletskoye region in the Altai Mountains (South Siberia) as revealed by apatite ssion-track thermochronology. Tectonophysics 349, 145–159, doi:10.1016/S0040-1951(02)00051-3.

Delvaux, D., 1993. The TENSOR programm for reconstruction: examples from East African and the Baikal rift systems. Terra Abstr., Abstr. Suppl. Terra Nova 5, 216.

Delvaux, D., Theunissen, K., Van der Meer, R., Berzin, N., 1995. Dynamics and paleostress of the Cenozoic Kurai-Chuya depression of Gorny-Altai (South Siberia): tectonic and climatic control. Russian Geol. Geophys. 36, N10, 26–45.

Delvaux, D., Moyes, R., Stapel, G., Petit, C., Levi, K., Miroshnitchenko, A., Ruzhich, V., Sankov, V., 1997. Paleostress reconstruction and geodynamics of the Baikal region, central Asia. Part II: Cenozoic rifting. Tectonophysics 282, 1–38.

Devyatkin, E.V., 1981. The Cenozoic of inner Asia (Stratigraphy, geochronology and correlation). In: Nikiforova (Ed.): The Joint Soviet-Mongolian Scientific-Research Geological Expedition. Transaction 27, 196 (in Russian).

Devyatkin, E.V., Malaeva, E.M., Zajigin, V.S. et al., 1989. Late Cenozoic of Mongolia (stratigraphy and paleogeography). In: Logatchov (Ed.): The Joint Soviet-Mongolian Scientific-Research Geological Expedition. Transaction 47, 213 p. (in Russian).

Guiraud, M., Laborde, O., Philip, H., 1989. Characterization of various types of deformation and their corresponding deviatoric stress tensor using microfault analysis. Tectonophysics 170, 289–316.

Heidbach, O., Reinecker, J., Tingay, M., Muller, B., Sperner, B., Fuchs, K., Wenzel, F., 2007. Plate boundary forces are not enough: Second- and third-order stress patterns highlighted in the World Stress Map database. Tectonics 26, TC6014, doi:10.1029/2007TC002133.

Hock, V., Daxner-Hock, G., Schmid, H.P., Badamgarav, D., Frank, W., Furtmuller, G., Montag, O., Barsbold, R., Khand, Y., Sodov, J., 1999. Oligocene- Miocene sediments, fossils and basalts from the Valley of Lakes (central Mongolia). An integrated study. Mitteilungen der Osterreichischen Geologishen Gessellschaft 90, 83–125.

Jolivet, M., Ritz, J.-F., Vassallo, R., Larroque, C., Braucher, R., Todbileg, M., Chauvet, A., Sue, C., Arnaud, N., De Vicente, R., Arzhanikova, A., Arzhanikov, S., 2007. Mongolian summits: an uplifted, fl at, old but still preserved erosion surface. Geology 35, N10, 871–874, doi:10.1130/G23758A.1.

Khilko, S.D., Kurushin, R.A, Kochetkov, V.M. et al., 1985. Earthquakes and base of seismic zoning of Mongolia. Moscow, Nauka, 224 p. (in Russian).

Mordvinova, V.V., Deschamps, A., Dugarmaa, T., Déverchère, J., Ulziibat, M., Sankov, V.A., Artemyev, A.A., Perrot, J., 2007. Velocity structure of the lithosphere on the 2003 Mongolian-Baikal transect from SV waves. Izv. RAS, Ser. Fizika Zemli 2, 21–32 (in Russian).

Nagibina, M.S., Schuvalov, V.F., Devyatkin, E.V. et al., 1975. Mesozoic and Cenozoic tectonics and magmatism of Mongolia, In: Yanshin (Ed.): The Joint Soviet-Mongolian Geological Expedition. Transactions 11, 308 p.(in Russian).

Parfeevets, A.V., Sankov, V.A., 2006. Crustal stress state and geodynamics of southwestern flank of Baikal rift system. Novosibirsk: Geo Academic Publishing House, 151 p. (in Russian).

Petit, C., Fournier, M., 2005. Present-day velocity and stress fields of the Amurian plate from thin-shell finite-element modelling. Geophys. J. Int. 160, 357–369.

Petit, C., Déverchère, J., Calais, E., San'kov, V., Fairhead, D., 2002. Deep structure and mechanical behavior of the lithosphere in the Hangay-Hövsgöl region, Mongolia: new constraints from gravity modelling. Earth Planet. Sci. Lett. 197, 133–149.

Ritz, J.-F., Bourle's, D., Brown, E.T., Carretier, S., Chery, J., Enhtuvshin, B., Galsan, P., Finkel, R.C., Hanks, T.C., Kendrick, K.J., Philip, H., Raisbeck, G., Schlupp, A., Schwartz, D.P., Yiou, F., 2003. Late Pleistocene to Holocene slip rates for the Gurvan Bulag thrust fault (Gobi-Altay, Mongolia) estimated with ^{10}Be dates. J. Geophys. Res. 108 (B3), 2162.

Sankov, V.A., Parfeevets, A.V., 2005. Late Cenozoic stress state in active fault zones of western Mongolia and Tuva. Doklady Akademii Nauk 403, N6, 796–800 (in Russian).

Sankov, V.A., Miroshnitchenko, A.I., Levi, K.G., Lukhnev, A.V., Melnikov, A.I., Delvaux, D., 1997. Cenozoic stress field evolution in the Baikal rift zone. Bull. Centre Rech. Elf Explor. Prod., Elf Aquitaine 21 (2), 435–455.

Sankov, V.A., Miroshnichenko, A.I., Parfeevets, A.V., Arzhannikova, A.V., Lukhnev, A.V., 2004. Late Cenozoic stress state of earth crust of Khubsugul basin (Northern Mongolia) by natural and experimental data. Geotectonika 2, 78–90 (in Russian).

Sankov, V.A., Lukhnev, A.V., Radziminovich, N.A., Melnikova, V.I., Miroshnichenko, A.I., Ashurkov, S.V., Calais, E., Déverchère, J., 2005. Quantitative estimation of the present-day crustal deformations of Mongolian block by GPS geodesy and seismotectonic data. Doklady Akademii Nauk 403, N5, 685–688 (in Russian).

Vassallo, R., Jolivet, M., Ritz, J.-F., Braucher, R., Larroque, C., Sue, C., Todbileg, M., Javkhlanbold, D., 2007a. Uplift age and rates of the Gurvan Bogd system (Gobi-Altay) by apatite fission track analysis. Earth Planet. Sci. Lett. 259, 333–346.

Vassallo, R., Ritz, J.-F., Braucher, R., Jolivet, M., Carretier, S., Larroque, C., Chauvet, A., Sue, C., Todbileg, M., Bourle's, D., Arzhannikova, A., Arzhannikov, S., 2007b. Transpressional tectonics and stream terraces of the Gobi-Altay, Mongolia. Tectonics 26, TC5013, doi:10.1029/2006TC002081.

Walker, R.T., Nissen, E., Molor, E., Bayasgalan, A., 2007. Reinterpretation of the active faulting in central Mongolia. Geology 35, 759–762.

Walker, R.T., Molor, E., Fox, M., Bayasgalan, A., 2008. Active tectonics of an apparently aseismic region: distributed active strike-slip faulting in the Hangay Mountains of central Mongolia. Geophys. J. Int. 174, 1121–1137.

Zonenshain, L.P., Savostin, L.A., 1981. Geodynamics of the Baikal Rift Zone and plate tectonics of Asia. Tectonophysics 76, 1–45.